Molecular Crystals and Liquid Crystals

Publication details, including instructions for authors and subscription information:
http://www.tandfonline.com/loi/gmcl20

Laser Beam Shaping using Self-Focusing in a Nematic Liquid Crystal

Andriy Shevchenko [a], Antti Hakola [a], Scott C. Buchter [a], Matti Kaivola [a] & Nelson V. Tabiryan [b]

[a] Department of Engineering Physics and Mathematics, Helsinki University of Technology, Espoo, Finland

[b] BEAM Engineering for Advanced Measurements Co., Winter Park, Florida, USA

Version of record first published: 22 Sep 2006

To cite this article: Andriy Shevchenko, Antti Hakola, Scott C. Buchter, Matti Kaivola & Nelson V. Tabiryan (2006): Laser Beam Shaping using Self-Focusing in a Nematic Liquid Crystal, Molecular Crystals and Liquid Crystals, 454:1, 217/[619]-224/[626]

To link to this article: http://dx.doi.org/10.1080/15421400600654348

Mol. Cryst. Liq. Cryst., Vol. 454, pp. 217/[619]–224/[626], 2006

ISSN: 1542-1406 print/1563-5287 online
DOI: 10.1080/15421400600654348

Taylor & Francis
Taylor & Francis Group

Laser Beam Shaping using Self-Focusing in a Nematic Liquid Crystal

Andriy Shevchenko
Antti Hakola
Scott C. Buchter
Matti Kaivola
Department of Engineering Physics and Mathematics,
Helsinki University of Technology, Espoo, Finland

Nelson V. Tabiryan
BEAM Engineering for Advanced Measurements Co.,
Winter Park, Florida, USA

A simple and efficient method to convert a Gaussian laser beam into a nearly non-diverging Bessel-like beam or into a thin-walled hollow beam is described. The optical system used for the beam conversion consists of a thin liquid-crystal cell and one or two lenses. At certain parameter values, self-focusing of a Gaussian beam directly results in the formation of a narrow Bessel-like beam, and, if an additional lens is used to collimate the self-focused beam, the collimated beam shows an accurate ring-shaped profile.

Keywords: Bessel beam; hollow beam; laser beam shaping; nematic liquid crystal; self-focusing

INTRODUCTION

Ordinarily, laser beams have a Gaussian spatial profile. In many applications, however, the radiation should be distributed in a specific, non-Gaussian way; in order not to lose the power, the desired field is created either by using appropriate laser resonators or by modifying a Gaussian beam with a certain spatial phase modulator. In this work we describe a simple method to convert a Gaussian beam into 1) a

Address correspondence to Andriy Shevchenko, Department of Engineering Physics and Mathematics, Helsinki University of Technology, P.O.B. 3500, 02015 Espoo, Finland. E-mail: andrej@focus.hut.fi

narrow and nearly non-diverging Bessel-like beam and 2) a thin-walled hollow beam. Such beams can be used in laser micromachining [1,2], trapping and guiding of micro- and nanoparticles or neutral atoms [3–6], precise optical alignment [7,8], and high-resolution imaging [9]. The beam conversion is accomplished by allowing the original Gaussian beam to undergo self-focusing in a thin nematic-liquid-crystal cell. The resulting light distribution is adjusted and properly shaped by using one or two lenses.

THEORY

The optical system we used is schematically shown in Figure 1. The lens L_1 is applied to adjust the Gaussian beam diameter on the crystal surface. The lens L_2 is used either as an imaging lens to image the Bessel-like beam profiles in the self-focal region behind the crystal onto the detector (see Fig. 1a), or as a collimating lens to collimate the self-focused beam when creating a hollow beam (see Fig. 1b). In order to simulate the field distribution in these beams, we use the Fresnel diffraction theory. We assume that the complex amplitude of the field in the plane of the crystal's back facet is known, $U(z = 0, \rho) \equiv U(0, \rho)$, with ρ being the distance from the beam axis, and write the Fresnel diffraction integral in cylindrical coordinates as [10].

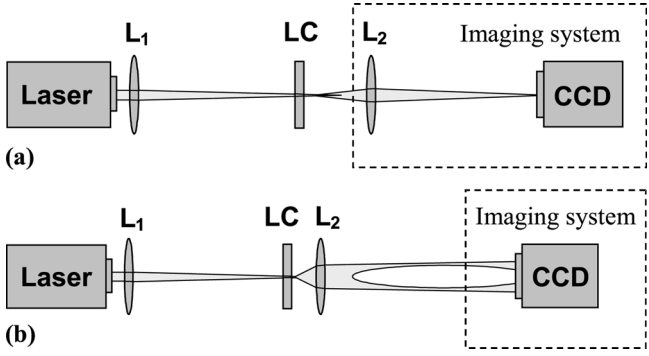

FIGURE 1 Experimental setup for creation of a Bessel-like beam (a) and a hollow beam (b). Lens L_1 is for adjustment of the beam diameter at the incident facet of the liquid crystal LC. In case (a), lens L_2 is translated together with the CCD array to create images of the Bessel-like beam profiles. In case (b) this lens is used to collimate the output beam. The images are taken directly with a CCD.

$$U(z,r) = \frac{2\pi}{\lambda z}\int_0^\infty U(0,\rho)\rho \exp\left(\mathrm{j}\frac{\pi\rho^2}{\lambda z}\right) J_0\left(\frac{2\pi r\rho}{\lambda z}\right) d\rho. \quad (1)$$

Here z denotes the distance from the crystal's back facet, r the distance from the beam axis in the observation plane, λ is the laser wavelength, and J_0 is the zeroth-order Bessel function of the first kind. The field $U(0,\rho)$ can be taken in the form

$$U(0,\rho) = \sqrt{I_p}\exp\left(-\frac{\rho^2}{W_{\mathrm{LC}}^2} + j\phi(\rho)\right), \quad (2)$$

where I_p is the peak intensity and W_LC the $1/e^2$ beam radius. The phase $\phi(\rho)$ due to self-phase modulation is given by

$$\phi(\rho) = \frac{2\pi}{\lambda} L n_2 I_\mathrm{p} \exp\left(-\frac{2\rho^2}{W_{\mathrm{LC}}^2}\right), \quad (3)$$

where L is the thickness and n_2 the equivalent nonlinear refractive index of the liquid crystal. In practice, the phase distribution $\phi(\rho)$ has a more complicated dependence on the parameters I_p, W_LC, n_2, and L, but this model still gives an accurate qualitative picture of the beam behavior [11–13]. Using Eq. (1) at $z > 0$, the complex amplitude $U(z,r)$ and the intensity $I(z,r) = |U(z,r)|^2$ of the field in the self-focal region can be calculated. On the other hand, one can evaluate the function $U(z,r)$ at negative z values. This function will describe the field which, propagating in free space, would result in the complex-amplitude distribution $U(0, \rho)$. When used to collimate the self-focused beam, the lens L_2 creates an image of this $U(z < 0, r)$-field in the form of a collimated hollow beam.

EXPERIMENTS

In the experiments we used a cw frequency-doubled Nd:YVO_4 laser operating at $\lambda = 532\,\mathrm{nm}$. A 100-μm thick, homeotropically oriented nematic liquid crystal with a nonlinear refractive index of $n_2 > 10^{-5}\,\mathrm{cm}^2/\mathrm{W}$ was inserted into the laser beam path. For creation of a Bessel-like beam, the radius W_LC of the beam inside the crystal was adjusted with the lens L_1 to be 220 μm (see Fig. 1a; the focal length of the lens is 200 mm). The lens L_2 (a 20× microscope objective) was positioned at a constant distance, 160 mm, from a CCD array (BeamStar FX 50). Several neutral-density attenuators were placed

between the lens and the CCD. The magnification of this imaging system was $M = 21.2$. By translating the whole imaging system ($L_2 + CCD$) at 500-μm steps along the optical axis, we recorder the profile of the self-focused beam. Near the focus, the beam profile has a strong central peak surrounded by a few much weaker rings. At certain values of W_{LC} and I_p, the width of this central peak becomes nearly constant over several millimeters along the beam path. The beam, therefore, behaves similarly to a Bessel beam in this range [14–18]. According to calculations based on Eq. (1), the parameter values $W_{LC} = 220\,\mu m$, $I_p = 1.7 \times 10^3\ W/cm^2$, and $n_2 = 3 \times 10^{-5}\,cm^2/W$ should result in a laser beam with a constant central peak width of about 5 μm for more than 5 mm beam length. Figure 2 shows both measured (left column) and calculated (right column) intensity profiles of the self-focused beam. The profile illustrated in Figure 2a is taken at a location close to the point where the beam intensity reaches maximum, and the profiles in Figures 2b and c are measured at distances of 1.5 mm and 4.5 mm from this point, respectively. The two-dimensional CCD images in the insets of Figure 2 illustrate the ring patterns of the beam. In Figure 2a, the beam $1/e^2$ radius is equal to 4.8 μm, and in Figures 2b and c, 5.8 μm and 9.8 μm, respectively. The spreading of the beam upon propagation is faster than that of the simulated beam, but it is still very slow compared to what it would be for a Gaussian beam. A Gaussian beam with the same waist size (4.8 μm) would have a $1/e^2$ radius of 160 μm at a 4.5-mm distance from the waist; its peak intensity would drop by a factor of 10^3, i.e., two orders of magnitude faster than the intensity of the beam in Figure 2.

For creation of a hollow beam, we used an essentially identical experimental setup (see Fig. 1b). This time, however, the lens L_2 is used to collimate the self-focused beam. For taking images, the CCD array was directly subjected to the illumination by the beam formed behind the lens. Figure 3 shows three measured intensity profiles of the beam created at a laser power of 195 mW (~30% above the measured self-focusing threshold). The profiles (a) and (b) are separated along the beam path by 4 mm, and (b) and (c) by 6 mm. The distance of the profile (b) from the lens L_2 (this time it is a 10× microscope objective) is 8 cm. The diameter of the light ring in this case is 960 μm, and the ring thickness is 30 μm (FWHM). As shown in Figure 3, the hollow beam intensity exceeds 1.5 times the peak intensity of the original Gaussian beam in the CCD plane, which implies an efficient confinement of the light in the ring profile. The power loss in the setup was measured to be 24% due to reflections of the beam at the glass-air interface in both the crystal cell and the objective. By changing the laser power P, the incident beam waist W_{LC}, and

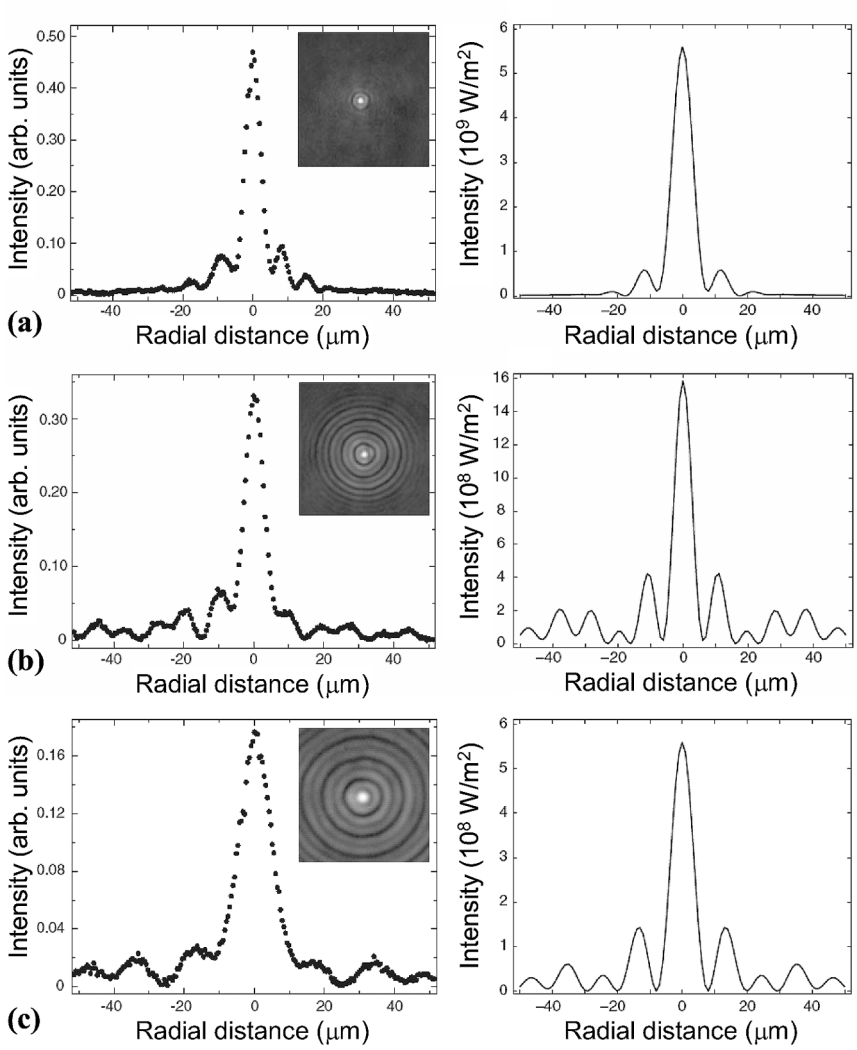

FIGURE 2 Spreading of a Bessel-like beam upon propagation; measured (left column) and corresponding simulated (right column) intensity profiles. The measured profile (a) has maximum peak intensity. The profiles (b) and (c) are taken at distances of 1.5 and 4.5 mm, respectively, from the position of the profile (a).

the distance between the crystal and the objective, we could adjust the diameter, size, and peak intensity of the hollow beam.

The origin of the formation of a hollow beam by the lens L_2 and the crystal is revealed by evaluating the integral in Eq. (1) for negative z

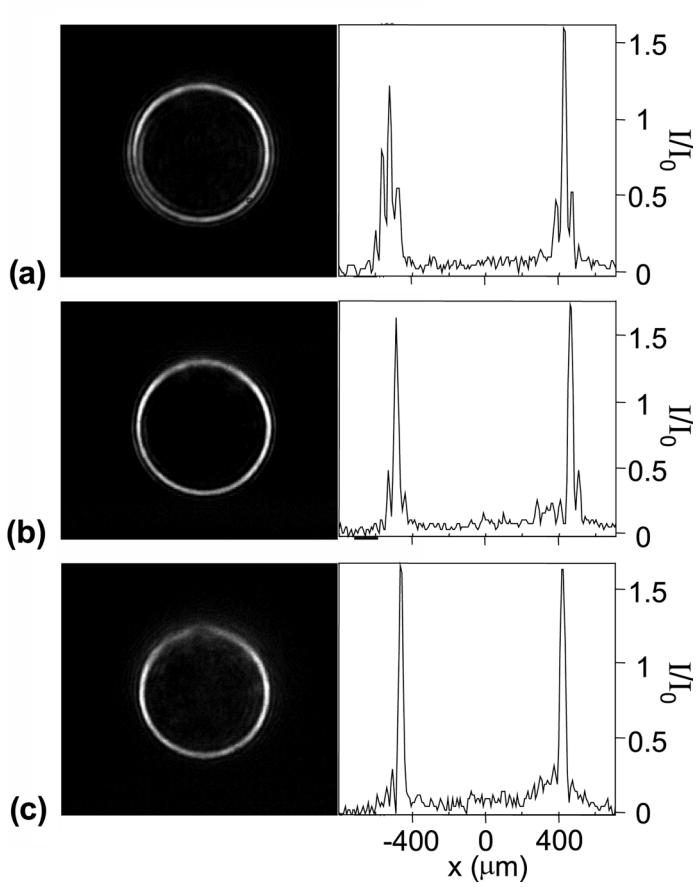

FIGURE 3 Transversal cross-sections of a hollow laser beam (on the left) and the corresponding intensity profiles along a horizontal line crossing the beam axis (on the right). Before reshaping, the Gaussian beam had a radius of $W_{LC} = 80\,\mu m$ in the crystal plane and $W_{CCD} = 370\,\mu m$ in the CCD plane. Its peak intensity in the CCD plane was $I_0 = 70\,W/cm^2$.

values. As shown in Figure 4, the calculated field is concentrated around a conical surface with the apex positioned on the optical axis. At the parameter values used to create the beam of Figure 3, and with $n_2 = 2.3 \times 10^{-5}\,cm^2/W$, the calculated virtual field has a ring-shaped transverse cross section with the ratio of the ring diameter to the ring thickness being equal to that of the profile (b) in Figure 3. The lens L_2 creates a magnified image of this profile, and, since the virtual field cone converges, the hollow beam becomes collimated when the cone apex lies in the front focal plane of the lens (see Fig. 4c).

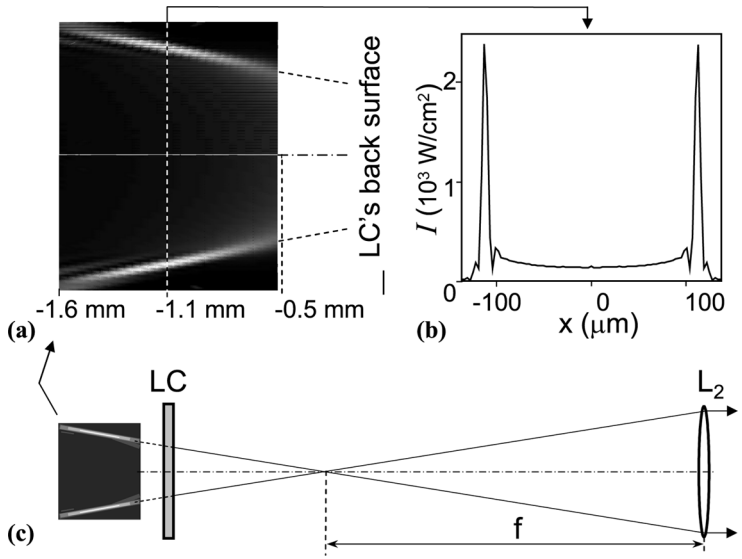

FIGURE 4 The calculated intensity profiles of the virtual field $U(z < 0, r)$ in a plane containing the optical axis (a) and in a perpendicular plane at $z = -1.1\,\text{mm}$ drawn along a radial direction (b). Figure (c) shows where the lens L_2 should be positioned to produce a hollow beam with constant diameter.

CONCLUSIONS

We have introduced a simple optical system that is able to create both a beam with a long and narrow focal line and a thin-walled hollow beam. It consists of a thin nematic-liquid-crystal cell and one or two lenses. The central-peak width of a Bessel-like beam can be made to stay below 10 micrometers over a propagation distance of several millimeters, which makes it superior over a Gaussian beam for applications, e.g., in laser micromachining or scanning imaging. The hollow beams can be made to have sub-millimeter diameters and a wall thickness of a few tens of microns for a propagation distance of about 10 mm. They can be made non-diverging, as well as diverging or converging. The optical system that is needed to produce beams of different sizes and peak intensities is simple and rather insensitive to the alignment of the optical elements (the beam is *a priorí* perfectly aligned with respect to the nonlinear lens it creates by itself). Finally, the system works equally well at different laser wavelengths.

REFERENCES

[1] Rioux, M., Tremblay, R., & Belanger, P.-A. (1978). *Appl. Opt.*, *17*, 1532.
[2] Charters, R. B., Luther-Davies, B., & Ladouceur, F. (1999). *IEEE Photon. Technol. Lett.*, *11*, 1617.
[3] Arlt, J., Garces-Chavez, V., Sibbett, W., & Dholakia, K. (2001). *Opt. Commun.*, *197*, 239.
[4] Lei, M. & Yao, B. (2004). *Opt. Commun.*, *239*, 367.
[5] Arlt, J., Hitomi, T., & Dholakia, K. (2000). *Appl. Phys. B*, *71*, 549.
[6] Florjanczyk, M. & Tremblay, R. (1989). *Opt. Commun.*, *73*, 448.
[7] Bickel, G., Häusler, G., & Maul, M. (1985). *Opt. Eng.*, *24*, 975.
[8] Jaroszewicz, Z., Climent, V., Duran, V., Lancis, J., Kolodziejczyk, A., Burvall, A., & Friberg, A. T. (2004). *J. Mod. Opt.*, *51*, 2185.
[9] Hausler, G. & Heskel, W. (1988). *Appl. Opt.*, *27*, 5165.
[10] Goodman, J. W. (1996). *Introduction to Fourier Optics*, The McGraw-Hill Companies, Inc.: Singapore.
[11] Wu, J. J., Chen, S. H., Fan, J. Y., & Ong, G. S. (1990). *J. Opt. Soc. Am. B*, *7*, 1147.
[12] Khoo, I. C., Hou, J. Y., Liu, T. H., Yan, P. Y., Michael, R. R., & Finn, G. M. (1987). *J. Opt. Soc. Am. B*, *4*, 886.
[13] Bolshtyansky, M. A., Tabiryan, N. V., & Zeldovich, B. Ya. (1997). *Opt. Lett.*, *22*, 22.
[14] McLeod, J. H. (1954). *J. Opt. Soc. Am.*, *44*, 592.
[15] McLeod, J. H. (1960). *J. Opt. Soc. Am.*, *50*, 166.
[16] Turunen, J., Vasara, A., & Friberg, A. T. (1988). *Appl. Opt.*, *27*, 3959.
[17] Vasara, A., Turunen, J., & Friberg, A. T. (1989). *J. Opt. Soc. Am. A*, *6*, 1748.
[18] Popov, S. Yu., Friberg, A. T., Honkanen, M., Lautanen, J., Turunen, J., & Schnabel, B. (1998). *Opt. Commun.*, *154*, 359.